K-edge x-ray absorption spectra of Cs and Xe

J. Padežnik Gomilšek
Faculty of Mechanical Engineering, Smetanova 17, SI-2000 Maribor, Slovenia

A. Kodre
Faculty of Mathematics and Physics, Jadranska 19, SI-1000 Ljubljana, Slovenia
and Jožef Stefan Institute, Jamova 39, SI-1000 Ljubljana, Slovenia

I. Arčon
Nova Gorica Polytechnic, Vipavska 13, SI-5000 Nova Gorica, Slovenia
and Jožef Stefan Institute, Jamova 39, SI-1000 Ljubljana, Slovenia

M. Hribar
Faculty of Education, Kardeljeva ploščad 16, SI-1000 Ljubljana
and Jožef Stefan Institute, Jamova 39, SI-1000 Ljubljana, Slovenia
(Received 28 May 2003; published 20 October 2003)

X-ray absorption spectrum of cesium vapor in the *K*-edge region is measured in a stainless steel cell. The spectrum is free of the x-ray absorption fine structure signal and shows small features analogous to those in the spectrum of the neighbor noble gas Xe. Although the large natural width of the *K* vacancy (>10 eV) washes out most of the details, fingerprints of multielectron excitations can be recognized at energies close to Dirac-Fock estimates of doubly excited states $1s4(d,p,s)$ and $1s3(d,p)$. Among these, the $1s3p$ excitation 1000 eV above the *K* edge in both spectra is the deepest double excitation observed so far. Within the *K*-edge profile, some resolution is recovered with numerical deconvolution of the spectra, revealing the coexcitation of the $5(p,s)$ electrons, and even the valence $6s$ electron in Cs. As in homologue elements, three-electron excitations, either as separate channels or as configuration admixtures are required to explain some spectral features in detail.

DOI: 10.1103/PhysRevA.68.042505 PACS number(s): 32.30.Rj, 32.80.−t

I. INTRODUCTION

The spectrometry of x-ray absorption edges and their vicinity provides information on the basic photoelectric ionization/excitation process in the atom and on the coexcitation of weakly bound electrons, revealed in the sharp small features (MPE—multielectron photoexcitations) in the smooth energy dependence of the photoelectric cross section above the edge [1]. The experiment requires the target element in the monatomic state, readily available only for noble gas elements. In the energy region above 3 keV, amenable to x-ray absorption spectrometry with a gas sample in a fixed cell, comprehensive edge and MPE data have been collected on the *K* edge of Ar [2], Kr [3–8], and Xe [9,10], and the *L* edges of Xe [11,12]. Some absorption edges in the lower energy region have been studied by other experimental techniques [13].

The atomic absorption spectrometry can be extended to monatomic vapors of metals. The technically demanding early experiments on nonvolatile metals like Cu and Ca yielded only the edge profiles [14]; the detection of the tiny MPE features remained beyond the sensitivity of the technique. Recent experiments on volatile alkaline-metal elements, however, have provided comprehensive MPE data, equivalent in resolution and sensitivity to the data on noble gases [15,16]. In fact, a simultaneous analysis of noble gas/alkaline-metal neighbor pairs Ar/K [15] and Kr/Rb [16] has been used to resolve specific coupling schemes and configuration mixing in the atoms.

In the present study of the *K*-edge spectra of Xe/Cs pair the main problem in the analysis is the large lifetime width. Although all the apparent spectral detail is washed out, some information can still be recovered by the use of comprehensive modeling and the recently introduced technique of natural-width deconvolution [17]. With these, many of the findings on MPE are explained with similar theoretical considerations as in homologue pairs.

There are no reports on the x-ray atomic absorption of cesium so far. The *K*-edge absorption of xenon has been studied before; there is a thorough study of the edge profile [9] and of the major MPE group of $K+N$ shell excitations [10]. Shortly after our preliminary report [18] of the present experiment with evidence of deep $K+M$ excitations the same observation was reported in another study [19].

II. EXPERIMENT

Cesium vapor was prepared in a stainless steel cell with stainless steel windows of 10-μm thickness. The cell and the tunnel oven, together with the details of the experiment, is the same as that described in the report on Rb [20]. The small amount of the metal in the sealed cell was completely vaporized at $\sim 610°$ C yielding a vapor pressure of 260 mbar.

The absorption experiment was performed at the X1 station of HASYLAB at the DORIS storage ring, using a two-crystal Si 311 monochromator. Its energy resolution of about

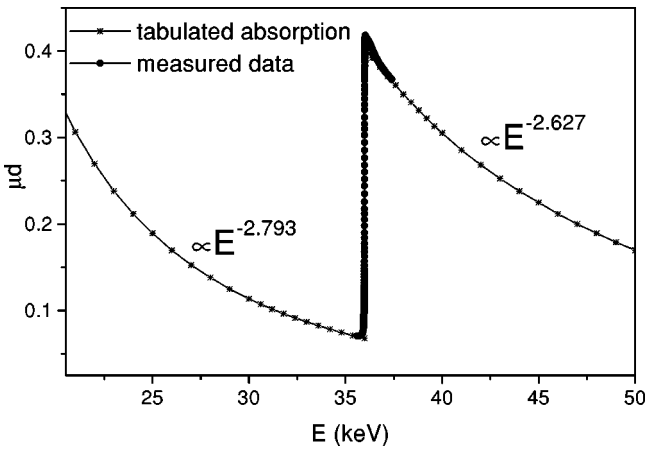

FIG. 1. Measured absorption in Cs on the background of tabulated absorption data. Victoreen exponents used in the analysis are shown.

7 eV at 35 keV contributes a negligible spread to the spectra with natural width of ~12 eV [21]. Owing to the high photon energy, the incident beam is free of harmonic contamination. The atomic absorption of Cs is derived from the difference in absorption on the heated and cold cell.

The absorption spectrum of xenon was measured in a conventional gas cell of 200 mm length with 0.5 mm thick perspex windows. The *K*-edge jumps of 0.3 and 2.4 for Cs and Xe, respectively, were obtained in measured spectra. With superposition of repeated scans, relative noise levels of 4×10^{-4} and 1×10^{-4} were achieved.

III. ANALYSIS

Prior to analysis the measured absorption spectra are normalized and provided with a precise energy calibration. The essential elements of the two steps are shown in Figs. 1 and 2. In the first step, the Victoreen formula ($\mu = A E^{-p}$) with asymptotic exponents determined from tabulated absorption data [22] far above and below the *K* edge (Fig. 1) is used to extract the normalized *K*-shell absorption a_K following the arguments and procedure in the Rb/Kr analysis [16]. The

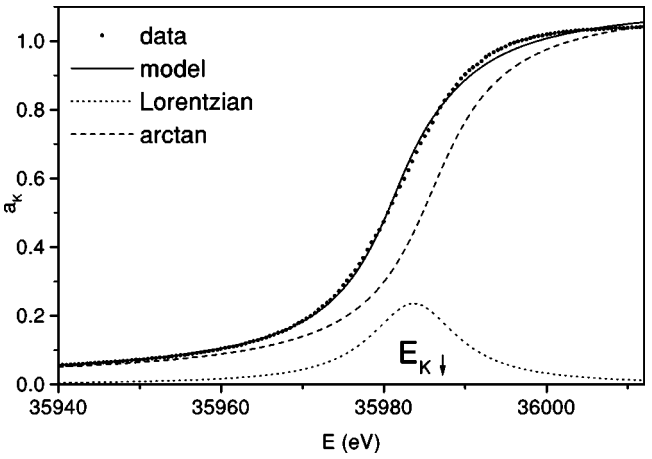

FIG. 2. The model of the Cs *K*-edge–determination of the threshold energy.

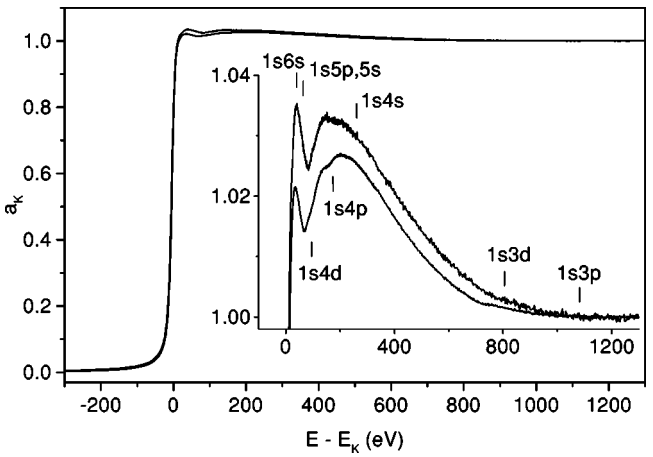

FIG. 3. Normalized absorption of Cs (above) and Xe (below). Dirac-Fock estimates for the lowermost excitations in each subshell group are indicated.

extracted a_K signal rises from zero to a value slightly above one at the *K* edge, and falls off slowly to one at the high-energy end (Fig. 3). In this way, the ambiguity of the edge jump definition, stemming from the variation of the edge profile with the chemical state of the sample and with the experimental resolution is avoided; a_K is normalized to the *K*-edge jump extrapolated from tabulated absorption data where the effects close to the edge are disregarded in the wide step. A similar reduction has been employed in the earlier study [10].

For the energy calibration, intrinsic definition of the energy scale has to be used as, basically, there is hardly any possibility of using an external standard. The drive of a modern monochromator is highly reliable, but the absolute precision required for the energy definition is seldom available. In the study of Deutsch *et al.* [9], the definition of a precise energy scale for Xe is extensively discussed. Two basic approaches are used to obtain the *K* ionization threshold energy: In the first one, a best-fit model of the preedge $[1s]6p$ resonance and the $[1s]$ edge is constructed on the experimental data and calibrated with the energy listed by Bearden and Burr [23]. In the second approach, the tabulated precision value of the characteristic Xe $K\alpha$ x-ray energy is combined with *L*-edges data of Breinig [24]. Both values agree to within 2 eV.

Teodorescu [25] studied the *K*-edge energies in noble gases and recognized Xe as a difficult problem. In the lighter homologues, he successfully applied the concept of the apparent absorption edge, shifted from the position of the proper continuum threshold by the accumulation of the unresolved lines in the Rydberg series of the preedge resonance. In Xe, however, because of the large natural width, even the leading preedge $[1s]6p$ resonance cannot be reliably separated from the $1s$ ionization edge.

In Cs, the singlet/triplet splitting of the resonance could modify the picture additionally. The calculation of the Dirac-Fock (DF) [26] energies of the edge resonance $[1s]6p$ requires the same orbital coupling and configuration interaction as in K and Rb. Specifically, the pure $[1s]6p$ configuration gives the triplet/singlet splitting of 1.8 eV.

However, the admixture of the $[1s6s]5d6p$ state reduces the splitting to ~ 0.7 eV, with a strongly dominant triplet $(6s6p\,^3P)1s$ component, so that a description with a single resonant term is sufficient.

Following Teodorescu's discussion, we build a quantitative model of the edge profile (Fig. 2) as a combination of a single Lorentzian resonance representing the compound $[1s]6p$ transition, and an arctan function representing the apparent edge at the $[1s]7p$ energy. Even in this simple model, the position of the apparent edge and the amplitude of the preedge resonance form a highly correlated parameter pair. A unique solution is only achieved with additional constraints: the energy difference of the components is kept fixed at the theoretical value, and the strength of the resonance relative to the edge jump at the common value found in the lighter homologue pairs. The point of the $[1s]$ threshold in the spectrum, to be used as the origin of the relative energy scale in the study of MPE, is obtained from the centroid of the $[1s]6p$ Lorentzian and the DF energy difference between the $[1s]6p$ state and the continuum of 2.3 and 3.5 eV, for Xe and Cs, respectively. Just for the purpose of comparison, the absolute energies of the $[1s]$ threshold are $E_K(\mathrm{Cs}) = 35\,987.2$ eV and $E_K(\mathrm{Xe}) = 34\,565.7$ eV, with the estimated uncertainty of 2 eV. The value for Xe lies within 1 eV of the value obtained by the second—and conceivably more reliable—approach by Deutsch *et al.* [9].

The resulting a_K absorption on the energy scale relative to the continuum threshold is shown in Fig. 3. In the inset, the above-edge portion of the spectrum is expanded. It shows clearly that immediately above the edge there are strong contributions to the absorption coefficient that are not encompassed in its asymptotic behavior. They extend to ~ 1000 eV above the edge. Their apparent amplitude of a few percent may hide a much higher true strength considering that they sit on a slowly rising edge profile; the large natural linewidth makes the arctangent profile saturate very slowly, reaching 96% at 50 eV and 99.8% at 1000 eV. These contributions, as seen in the inset of Fig. 3, start with an overshoot of 2% and 3.5% for Xe and Cs, respectively, of the normalized edge, continuing in a smooth decay towards the asymptotic value of one, interrupted by another sharp rise at ~ 80 eV. The rise and other smaller sharp features in the spectrum appear in the vicinity of the Dirac-Fock estimates of the energy intervals of double excitations indicated in Fig. 3.

The slowly decaying overshoot of the normalized edge has been recognized in several noble gases and has been generally attributed to the core relaxation (CR) [27] and postcollision interaction (PCI) [28]. In the asymptotic region far above the photoeffect threshold, the ejection of the fast photoelectron can be treated in the sudden approximation, decoupled from the relaxation of the excited atom. Just above the threshold, however, the slow photoelectron is affected by the rearrangement of atomic electrons and by subsequent Auger emission and the probability of its ejection is modified. Deutsch *et al.* [9] give estimates of the energy range of the effect in Ar, Kr, and Xe and show that, specifically for Xe, the PCI contribution is negligible. In our approach introduced in the Rb/Kr analysis, the entire CR/PCI contribution is approximated with a simple exponential ansatz, $A\,e^{-\alpha E}$. For Xe and Cs, the best-fit procedure yields the decay constants $1/\alpha$ of 260 and 280 eV, respectively, in accord with the apparent total range of 600 eV for Xe given in Ref. [9]. After the removal of the ansatz, the MPE contribution is revealed (Fig. 4) as a sequence of slowly saturating shake-off profiles. Even the weak $1s3d$ excitation is clearly discernible far out beyond the much stronger $1s4(d,p,s)$ MPE feature. The resonances from double bound-bound transitions, however, well resolved in the lighter homologues, are smeared out by the large linewidth.

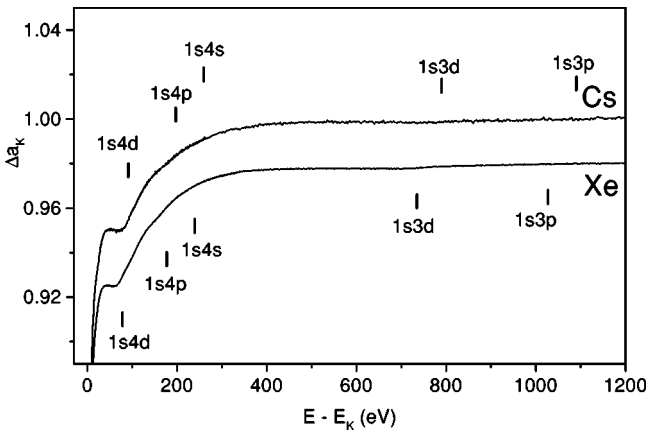

FIG. 4. Reduced absorption in Xe and Cs after removal of the exponential ansatz showing the consecutive MPE contributions. Xe signal is shifted by -0.02 along y axis.

It should be noted that the tail of the edge profile is also absorbed into the ansatz, providing an effective baseline to the deeper MPE features further out from the edge, as evident from Fig. 4. In the region of the valence MPE features, however, both contributions are large and a simple form for the sum cannot be surmized.

A. $1s6s$, $1s5p$, and $1s5s$ excitations

The valence and subvalence coexcitations contribute finely detailed features in the spectra of the lighter homologues; in Xe and Cs they lie within 50 eV above the edge and are all hidden in the saturation of the edge profile (Fig. 5). However, the deconvolution procedure introduced by Filipponi [17] sharpens the edge and reveals that it rises to a much larger overshoot ($\sim 15\%$). A distinct knee appears in the middle of its descending high-energy side at ~ 20 eV. Another feature is an additional bump at the top of the deconvoluted Cs edge, a candidate for the $1s6s$ MPE, recognized in the comparison of the Cs and Xe spectra.

It is worth noting that the dramatic increase of the overshoot in the deconvolution may not yet be the final result since the noise level of the measured spectra only allows about two-third of the natural width to be removed in the deconvolution procedure. This means that the true amplitude of the CR contribution and also of the valence and subvalence excitations exceeds the values suggested in Fig. 5. In this view, the large values of 12% and 1.7% for the $5p$ and $5s$ shake, respectively, by Carlson and Nestor [29] may be entirely realistic. Any estimate of these amplitudes from the experimental data, however, is unreliable, since the true en-

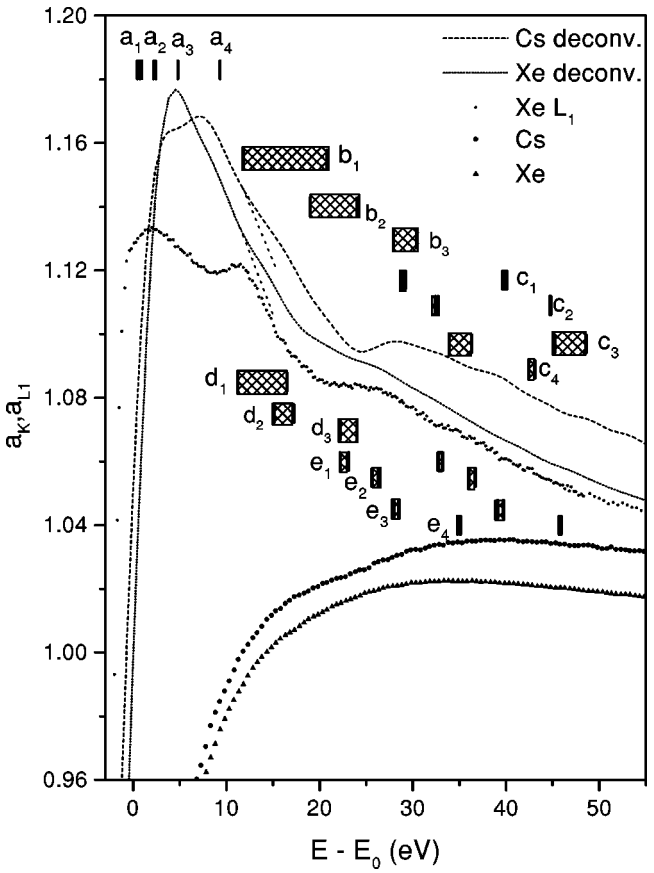

FIG. 5. Deconvolution of the Xe and Cs K absorption and comparison with Xe L_1 absorption. The a_K spectra below as in Fig. 3. No vertical shift is introduced. The change of slope at the onset of the $1s5p$ channel is indicated by a dotted line. DF multiplet intervals for Cs (a,b,c) and Xe (d,e): a_1, $[1s6s]7s6p$; a_2, $[1s6s]6p$; a_3, $[1s6s]7s$; a_4, $[1s6s]$; b_1,d_1, $[1s5p](6p^2+5d^2)$; b_2,d_2, $[1s5p]6p$; b_3,d_3, $[1s5p]$; c_1, e_1, $[1s5s]6s6p$; c_2,e_2, $[1s5s]6s$; c_3,e_3, $[1s5s]6p$; c_4, e_4, $[1s5s]$. The CI in the c and e multiplets is discussed in text.

ergy dependence of the CR contribution is not known, and the extrapolation of the average exponential ansatz to the large values immediately above the edge is not justified.

As an exception, the $1s6s$ MPE feature, present only in Cs, may be reliably estimated, using the spectrum of Xe as a baseline. Among the main excitation channels $[1s6s]6p7s$, $[1s6s]6p$, $[1s6s]7s$, and $[1s6s]$ (a_1–a_4 energy intervals in Fig. 5) the DF energy of the $[1s6s]7s$ shake-up lies closest to the apparent onset of the $1s6s$ feature. The valence-electron shake-up is the strongest contribution to the feature also in all lighter homologues. The combined strength of the $6s$ coexcitation in Cs is estimated to $\sim 2\%$ of the K edge from the difference between Cs and Xe spectra.

The structure of $1s5p$ and $1s5s$ MPE groups, observed in both elements, is more complex. In the identification of excitation channels the comparison with Xe L_1 absorption spectrum [12] provides additional information. The coexcitation of the valence electron is expected to be rather insensitive, apart from the difference in natural widths, to the principal quantum number of the core s hole. Indeed, beyond

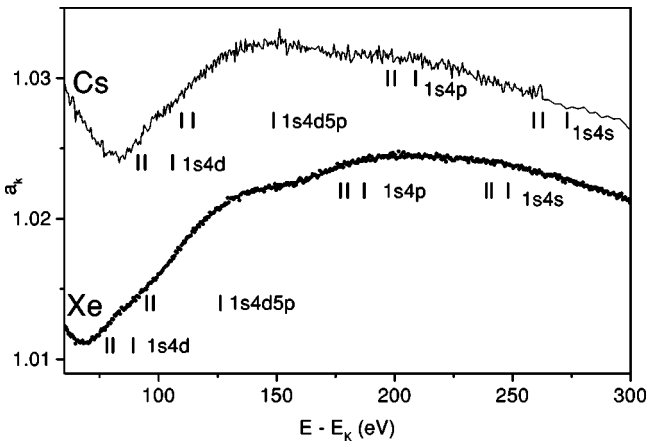

FIG. 6. N shell coexcitations in Cs and Xe, with HF multiplet averages for resonant, shake-up, and shake-off transitions.

~ 15 eV of the relative energy scale, the deconvoluted Xe K spectrum and the Xe L_1 spectrum show a perfect agreement (Fig. 5). There is, however, in the L_1 spectrum, a bump at ~ 12 eV, identified as $2s5p$ resonance, for which the counterpart in the K spectrum is only a slight break in the steep slope at the same relative energy, matching the configuration interaction (CI) multiplet $[1s5p](6p^2,5d^2)$ (d_1 interval). A strong mixing of corresponding states is found in lighter homologues [15,16]. The first state arises in a double excitation ($1s\rightarrow 6p$, $5p\rightarrow 6p$), and the second one in a single $1s\rightarrow 5p$ transition from a $\sim 4\%$ admixture $[5p^2]5d^2$ to the ground state.

The break of slope at 20 eV is, analogously with the feature in the L_1 spectrum, identified as $1s5s$ transition (and not as $1s5p$ shake-off as one might guess at the first sight). Although the range of the $1s5s$ resonance multiplet in the single configuration DF calculation starts well beyond the onset of the feature, a CI admixture of the $[1s5p^2]5d6p6s$ state splits the multiplet in the ratio of 3:2 into two groups of levels ~ 10 eV apart (c_1 and e_1 in Fig. 5); the energy of the lower group is ~ 4.5 eV below the single configuration result, coinciding with the onset in the spectrum. A similar splitting is found in the $2s5s$ excitation at Xe L_1 and in s-subshell valence coexcitations in lighter homologues. The mixing of $[5s]^2S$ and $[5p^2]5d^2S$ improves the description of the $5s$ hole and can also be observed in $1s5s$ shake-up and shake-off states (intervals c_2–c_4 and e_2–e_4). The apparent relative strength of the $5p$ and $5s$ coexcitations is misleading: the presumably much stronger $1s5p$ feature is hidden in the steep CR slope, while the $1s5s$ feature protrudes from a region of a gentler slope.

B. $1s4(d,p,s)$ excitations

The fingerprints of the coexcitations in the N subshells can be observed directly (Fig. 6) and have already been identified in Xe absorption [10]. The overall shape of the feature is determined by the channels of $4d$ coexcitation; the apparent threshold of the $4p$ shake can be recognized as a change of slope in both Xe and Cs, and the onset of the $4s$ coexcitation is barely noticeable in Xe. The relative noise level is

so high that no improvement in resolution can be expected from the deconvolution procedure. In quantitative modeling, however, the inclusion of "hidden" contributions may be necessary for a successful fit.

The Hartree-Fock (HF) [30] energies of multiplet averages of lowermost resonant, shake-up and shake-off channels, shown in Fig. 6 as short vertical lines lie regularly 10–20 eV above the observed subshell thresholds. In view of the large natural width, the explanation is the same as in the case of the single-electron excitation in the *K* edge; the unresolved Rydberg resonances pile up in front of the continuum threshold and shift its apparent position to lower energy. Since not even the lowermost resonance is resolved, the apparent threshold may be found approximately one linewidth below its HF estimate. The onset of the $1s4p$ vacancy states for both elements is shifted from a HF estimate toward lower energies for additional 10 eV as a consequence of strong mixing of the $[4p]$ vacancy with the $[4d^2]4f$ states [31]. The mixing depends on *j*-value; the $4p_{3/2}$ multiplet is split into a lower group 10 eV below the unmixed multiplet average and a higher group 20 eV above it, with the intensity ratio 2:1. The $4p_{1/2}$ levels show the same picture shifted for 10 eV but with the reversed ratio.

Thus, a model is constructed with constrained $4(d,p,s)$ shake components: arctan profiles for the shake-up and exponential saturation for the shake-off channels; the analytic forms are given explicitly in [16]. A shift in the energy threshold parameters is introduced to take into account the contribution of the neglected resonant terms. Constraints are placed on width parameters and relative energies. The range of the exponential shake-off terms is fixed at 40% of the relative threshold energy as in the Rb case. The model shows unambiguously that the terms are not sufficient to describe the observed spectral feature. Additional shake components are required in the energy interval between $1s4d$ and $1s4p$ excitations; a similar case is known from the Kr/Rb homologues where a substantial contribution from three-electron excitations of the $1s3d4p$ type is found. In Xe, the three-electron $1s4d5p$ contribution is even stronger; it is shown in Fig. 7 as a residue after removal of two-electron contributions. Its presence is explained in the same way as in the lighter homologues with an admixture of a valence $[p^2]d^2$ excitation to the ground state. The three-electron channel is then realized as a double-electron transition (e.g., $1s\rightarrow 5p$, $4d\rightarrow 5d$ for the leading resonant excitation) from the admixed component of the ground state.

For transition probabilities only the theoretical value for the total shake in the *N* shell (5.4%) has been determined for Xe [29]. This is also the probability that can be most reliably determined from the experimental data. Our value of 6.0% stands in good agreement, but considerably higher than the value 1.9% from the experiment of Deutsch and Kizler [10]. This is undoubtedly the consequence of the different treatments of the spectra, specifically, of a different model of the smooth baseline beneath the MPE features. The total *N* shake probability for Cs is estimated to be 5.6%.

C. $1s3(d,p)$ excitations

Owing to the careful treatment of the smooth contributions in the absorption and the signal-to-noise ratio of better than 10^4, a slight bend can be isolated in the Xe spectrum at the relative energy of 740 eV (Fig. 8). It introduces a long saturation profile with a range of ~300 eV. The steep initial rise, however, indicates also a shake-up contribution. Its large width is a combination of the natural width and the $d_{3/2}$-$d_{5/2}$ splitting of ~15 eV. The amplitudes of the components are strongly correlated and thus unreliable; however, a robust estimate can be obtained for the total shake amplitude. The value of $0.4\pm 0.1\%$ is close to the theoretical value 0.54% of Carlson and Nestor [29], at least in comparison with the upper limit estimate of 0.05% from the experiment of Deutsch and Kizler [10]. Further out at the energy of ~1050 eV, another tiny bend in the smooth slope can be interpreted as a vestige of the $1s3p$ excitation group, too weak against the noise to allow extraction of any meaningful quantitative data. Its contribution, however, may be demonstrated (Fig. 8) in a plot of the $1s3d$ shake model fitted to the

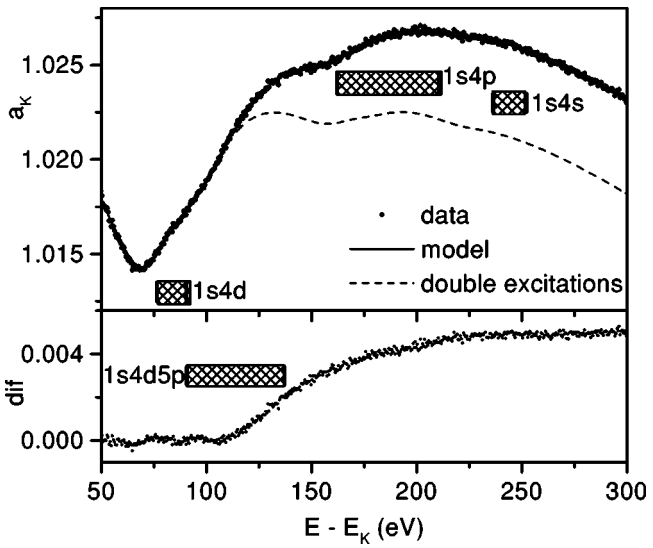

FIG. 7. Triple excitation in the $1s4d$ feature of Xe. DF multiplet intervals are shown, with the large CI effect in $1s4p$ (see text).

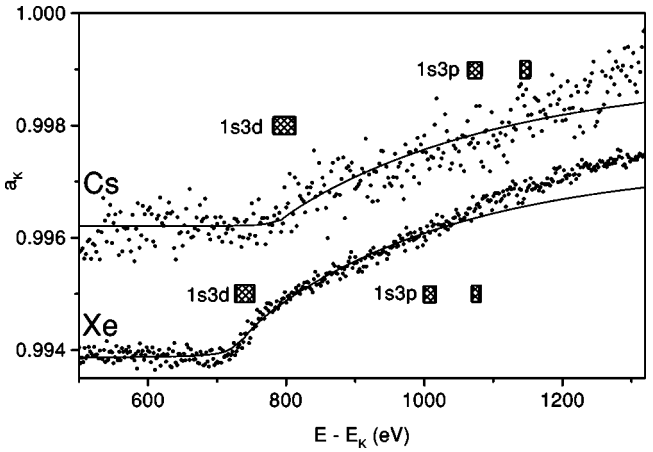

FIG. 8. Coexcitation of the *M* shell. The Xe spectrum is shifted for -0.0018 along *y* axis for clarity. The span of the single-configuration DF multiplets for shake-up and shake-off is indicated. Note the large *j*-splitting in the $1s3p$ multiplets.

data within 300 eV above the threshold. Similarly, the larger noise in the Cs spectrum makes the $1s3d$ excitation barely visible, allowing a crude estimate of the total shake probability of 0.3%.

IV. CONCLUSIONS

The pure *K*-edge atomic absorption spectrum of Cs is measured for the first time. As in other metals, the monatomic nature of the vapor is presumed, although the presence of Cs dimers is amply documented in optical spectroscopy. The Cs_2 component would be clearly recognized in the absorption for its specific EXAFS (extended x-ray absorption fine structure) harmonic signal of very short period, due to the large interatomic radius, as in the random Cs/Na alloy [32]. From the absence of this signal the upper limit of the dimer concentration in our spectra is estimated at 10^{-3}, far below the equilibrium value, calculated from the binding energy of the molecule. This equilibrium is never attained, since the dimers are readily destroyed but, for kinetic reasons, cannot be created, in binary collisions. They are predominantly formed at the walls, and efficiently destroyed in the high-temperature and high-density vapor in our experiment.

When the Cs spectrum is compared to the remeasured absorption spectrum of Xe gas, the similarities of MPE features in both elements are fully evident. The small but informative differences in the corresponding features, found in the lighter homologue pairs Rb/Kr and K/Ar, here remain obscured by the noise and the large natural width. The similarity with the homologues is invoked in establishing the proper energy calibration, i.e., in the determination of the *K* binding energy which has been recognized as a difficult problem. The similarity is exploited also in the exponential ansatz which helps to properly resolve the groups of the MPE features. Thus, the applicability of this heuristic approach is now tested on a wide range of elements with the decay constants of the exponential spread over an order of magnitude.

The estimates of the shake probabilities, using the ansatz as the smooth baseline of the features, agree well with the theoretical estimates for Xe, but not so well with the earlier experimental values, precisely for the different treatment of the baseline. The corresponding experimental values for Cs tend to be slightly lower than those for Xe.

The analysis of MPE in the heaviest noble gas/alkaline-metal pair for which the absorption spectrometry experiment is practically feasible cannot produce the rich multiplet detail of lighter homologues. However, the accessible depth of the coexcitation is larger so that the coexcitations of the same orbital momentum in subshells with different principal quantum numbers can be compared in a single experiment.

The considerable strength of the excitations to the triple vacancy $1s4d5p$ states bears witness to the ground-state configuration mixing with the $[5p^2]5d^2$ states. The rather constant strength of the admixed configuration ($\sim 4\%$) in the homologue pairs opens up the question whether the mixing is universal or specific to the vicinity of closed-shell elements. Calculations in the DF model show that the inclusion of the admixture is generally beneficial to the description of the ground state; however, its amplitude is particularly large in elements with a filled *p* subshell and completely empty *d* subshell with small excitation energy.

Two other mixing combinations are found: the final-state CI description of the $[5s]$ and $[4p]$ vacancy states with the admixture of the double vacancy states of the higher orbital momentum, $[5p^2]5d$ and $[4d^2]4f$, respectively. The induced splitting is found in all three types of reaction channels, witnessing that the mixing arises from the polarization of the coexcited vacancy, not from the interaction of some specific outer orbitals. The first case has its counterpart also in the lighter homologues, the second, involving *f* orbitals, can only arise in the Xe neighborhood.

ACKNOWLEDGMENTS

The work was supported by Slovenian Ministry of Education, Science, and Sport, Internationales Büro des BMBF (Germany) and IHP-Contract HPRI-CT-1999-00040 of the European Commission. Advice on beamline operation by L. Tröger and N. Haack of HASYLAB is gratefully acknowledged.

[1] A. Kodre, S.J. Schaphorst, and B. Crasemann, in *X-ray and Inner-Shell Processes*, edited by T. A. Carlson, M. O. Krause, and S. T. Manson, AIP Conf. Proc. 215 (AIP, New York, 1990), p. 582.
[2] R.D. Deslattes, R.E. LaVilla, P.L. Cowan, and A. Henins, Phys. Rev. A **27**, 923 (1983).
[3] S.J. Schaphorst, A.F. Kodre, J. Ruscheinski, B. Crasemann, T. Åberg, J. Tulkki, M.H. Chen, Y. Azuma, and G.S. Brown, Phys. Rev. A **47**, 1953 (1993).
[4] E. Bernieri and E. Burattini, Phys. Rev. A **35**, 3322 (1987).
[5] Y. Ito, H. Nakamatsu, T. Mukoyama, K. Omote, S. Yoshikado, M. Takahashi, and S. Emura, Phys. Rev. A **46**, 6083 (1992).
[6] M. Deutsch and M. Hart, Phys. Rev. A **34**, 5168 (1986).
[7] M. Deutsch and M. Hart, Phys. Rev. Lett. **57**, 1566 (1986).
[8] M. Deutsch and M. Hart, J. Phys. B **19**, L303 (1986).
[9] M. Deutsch, G. Brill, and P. Kizler, Phys. Rev. A **43**, 2591 (1991).
[10] M. Deutsch and P. Kizler, Phys. Rev. A **45**, 2112 (1992).
[11] K. Zhang, E.A. Stern, J.J. Rehr, and F. Ellis, Phys. Rev. B **44**, 2030 (1991).
[12] I. Arčon, A. Kodre, M. Štuhec, D. Glavič-Cindro, and W. Drube, Phys. Rev. A **51**, 147 (1995).
[13] J.M. Esteva, B. Gauthé, P. Dhez, and R.C. Karnatak, J. Phys. B **16**, L263 (1983).
[14] U. Arp, B.M. Lagutin, G. Materlik, I.D. Petrov, B. Sonntag, and V.L. Sukhorukov, J. Phys. B **26**, 4381 (1993).
[15] J.P. Gomilšek, A. Kodre, I. Arčon, and R. Prešeren, Phys. Rev. A **64**, 022508 (2001).

[16] A. Kodre, I. Arčon, J. Padežnik Gomilšek, R. Prešeren, and R. Frahm, J. Phys. B **35**, 3497 (2002).
[17] A. Filipponi, J. Phys. B **33**, 2835 (2000).
[18] J. Padežnik Gomilšek, R. Prešeren, A. Kodre, I. Arčon, and M. Hribar, in *Hamburger Synchrotronstrahlungslabor HASYLAB am Deutschen Elektronen-Synchrotron DESY: Jahresbericht 1999* (Hamburg: Hamburger Synchrotronstrahlugslabor HASYLAB at Deutsches Elektronen-Synchrotron DESY, 1999), p. 205.
[19] Y. Ito, T. Tochio, K. Mutaguchi, H. Ohashi, N. Shigeoka, Y. Nakata, A.M. Vlaicu, T. Uruga, S. Emura, and J. Padežnik Gomilšek, Radiat. Phys. Chem. **61**, 405 (2001).
[20] R. Prešeren, I. Arčon, M. Mozetič, A. Kodre, and A. Pregelj, Nucl. Instrum. Methods Phys. Res. B **111**, 161 (1996).
[21] M.O. Krause and J.H. Oliver, J. Phys. Chem. Ref. Data **8**, 329 (1979).
[22] M. J. Berger, J. H. Hubbell, S. M. Seltzer, J. S. Coursey, and D. S. Zucker, in XCOM: *Photon Cross Section Database*, version 1.2, Online, 1999, http://physics.nist.gov/xcom, National Institute of Standards and Technology, Gaithersburg, MD, 2002.
[23] J.A. Bearden and A.F. Burr, Rev. Mod. Phys. **39**, 126 (1967).
[24] M. Breinig, M.H. Chen, G.E. Ice, F. Parente, B. Crasemann, and G.S. Brown, Phys. Rev. A **22**, 520 (1980).
[25] C.M. Teodorescu, R.C. Karnatak, J.M. Esteva, A. El Afif, and J.-P. Connerade, J. Phys. B **6**, 4019 (1993).
[26] K.G. Dyall, I.P. Grant, C.T. Johnson, F.A. Parpia, and E.P. Plummer, Comput. Phys. Commun. **55**, 425 (1989).
[27] J. Tulkki and T. Åberg, J. Phys. B **18**, L489 (1985).
[28] M.Y. Amusia, V.K. Ivanov, and V.A. Kupchenko, J. Phys. B **14**, L667 (1981).
[29] T.A. Carlson and C.W. Nestor, Phys. Rev. A **8**, 2887 (1973).
[30] C. Froese-Fischer, Comput. Phys. Commun. **43**, 355 (1987).
[31] G. Wendin and M. Ohno, Phys. Scr. **14**, 148 (1976).
[32] I. Arčon, A. Kodre, J. Padežnik Gomilšek, M. Hribar, and M. Mihelič, Phys. Scr. (to be published).